

$\frac{1}{2}^+ \rightarrow \frac{1}{2}^+$ beta decay with neutrino mass effects
in the elementary particle treatment of weak interactions

Chong-en Wu*

*Guangxi University, Nanning, Guangxi, People's Republic of China
and Department of Physics and Astronomy, Michigan State University, East Lansing, Michigan 48824*

Wayne W. Repko

Department of Physics and Astronomy, Michigan State University, East Lansing, Michigan 48824

(Received 2 August 1982)

We compute the effect of a nonvanishing neutrino mass on the electron spectrum of tritium beta decay using the elementary particle treatment of weak interactions. Coulomb corrections are taken into account in this formalism, as are the effects of weak magnetism and nuclear recoil. The effect of a mixture of excited atomic final states is also discussed. These corrections combine to make small changes in the shape of the end point, which could be important in determinations of the neutrino mass.

[RADIOACTIVITY Calculation of neutrino mass and Coulomb effects]
on the spectrum of ^3H β decay.

I. INTRODUCTION

Precise measurements of the tritium (^3H) beta decay end point using a gas of atomic ^3H are being undertaken¹ in an effort to measure the neutrino mass, m_ν . The gaseous source technique is free from possible complications associated with the chemical environment of the ^3H . It therefore provides an attractive alternative to end point experiments in condensed matter systems,² which report a value $m_\nu = 35$ eV.

Since extraction of the neutrino mass requires a comparison of the experimental data with a theoretical spectrum, and the effect is small, we have reexamined the theoretical spectrum using the elementary particle approach.³ In particular, we have included Coulomb corrections by employing the technique of Armstrong and Kim.⁴ We use wave functions for an electron moving in the field of a uniformly charged nucleus. These wave functions agree very well with existing tables⁵ for all values of the electron momentum. The effect of weak magnetism is also considered. We find that weak magnetism contributes at the level of a few parts in 10^4 . Detailed plots of the end point shape for the ground state and

first atomic excited state are presented. We also present a simple algebraic description of the Kurie plot which represents our calculation very accurately near the end point. These results, which include the effects of nuclear recoil and atomic excitations of the final state, should be relevant to the analysis of experimental beta decay data. For a complete understanding of the beta spectrum, it is necessary to include the effects of real photons on the electron distribution. We are currently investigating this radiative process.

Section II contains the formalism relevant to tritium beta decay. This is followed by a development of the electron wave function for the case of a uniformly charged nucleus. In Sec. IV, we discuss the evaluation of the transition rate, and in Sec. V we present the results for the electron spectrum and the Kurie plot.

II. FORMALISM FOR $\frac{1}{2}^+ \rightarrow \frac{1}{2}^+$ DECAYS

In the elementary particle approach to nuclear beta decay, the transition amplitudes are expressed as

$$\mathcal{M} = \frac{G \cos\theta_c}{\sqrt{2}} (2\pi)^3 \delta^{(3)}(\vec{p}_i - \vec{p}_f - \vec{p}_e - \vec{p}_\nu) \langle f(\vec{p}_f) | J_\alpha^{(+)}(0) | i(\vec{p}_e) \rangle_0 \langle \bar{\psi}_e \rangle \gamma_\alpha (1 + \gamma_5) v_\nu(\vec{p}_\nu), \quad (1)$$

$$\begin{aligned}
\langle f | J_{\alpha}^{(+)}(0) | i \rangle &= \langle f | V_{\alpha}^{(+)}(0) | i \rangle + \langle f | A_{\alpha}^{(+)}(0) | i \rangle , \\
\langle f | V_{\alpha}^{(+)}(0) | i \rangle &= \bar{u}_f \left[\gamma_{\alpha} F_V(q^2; i \rightarrow f) - \frac{\sigma_{\alpha\beta} q_{\beta}}{2m_p} F_M(q^2; i \rightarrow f) \right] u_i , \\
\langle f | A_{\alpha}^{(+)}(0) | i \rangle &= \bar{u}_f \left[\gamma_{\alpha} \gamma_5 F_A(q^2; i \rightarrow f) + \frac{i(m_i + m_f)}{m_{\pi}} q_{\alpha} \gamma_5 F_P(q^2; i \rightarrow f) \right] u_i .
\end{aligned} \tag{2}$$

Here, $J_{\alpha}^{(+)}$ denotes the charge raising current, with $V_{\alpha}^{(+)}$ and $A_{\alpha}^{(+)}$ its vector and axial vector parts. G_F is the Fermi constant, m_p the proton mass, and θ_C the Cabibbo angle. The quantities F_V , F_M , F_A , and F_P are, respectively, the vector, weak magnetic, axial vector, and pseudoscalar form factors. The Fourier transforms of these form factors are related to the corresponding structure functions as

$$F_i(q^2) = \int \rho_i(\vec{x}) e^{i\vec{q}\cdot\vec{x}} d\vec{x} , \tag{3}$$

with the F_i written as

$$F_i(q^2) = F_i(0) \mathcal{F}_i(q^2) , \tag{4}$$

where the $\mathcal{F}_i(q^2)$ are normalized form factors. It can be shown that the normalized form factors have approximately the same q^2 dependence:

$$\mathcal{F}_V(q^2) = \mathcal{F}_A(q^2) = \mathcal{F}_M(q^2) \equiv \mathcal{F}(q^2) . \tag{5}$$

F_P does not have this q^2 dependence, but this term is much smaller than the others and will be neglected in what follows. A normalized structure function $\phi(x)$ corresponding to $\mathcal{F}(q^2)$ may also be introduced as

$$\begin{aligned}
\mathcal{F}(q^2) &= \int \varphi(\vec{x}) e^{i\vec{q}\cdot\vec{x}} d\vec{x} , \\
\int \varphi(\vec{x}) d\vec{x} &= 1 .
\end{aligned} \tag{6}$$

Note that the subscript zero in Eq. (1) implies that q^2 is taken to be zero in the matrix elements of $J_{\alpha}^{(+)}(0)$. The values of $F_i(0)$ are taken to be⁶

$$F_V = 1.00, \quad F_A = 1.22, \quad F_M = -6.106 , \tag{7}$$

where F_M is calculated from the values of the magnetic moments of ${}^3\text{H}$ and ${}^3\text{He}$, namely

$$\mu({}^3\text{H}) = 2.9789 \text{ nm}, \quad \mu({}^3\text{He}) = -2.1276 \text{ nm}$$

using the conserved vector current (CVC) hypothesis.⁶

If the electron wave function is denoted by ψ_e , then

$$\langle \bar{\psi}_e \rangle = \int d\vec{r} \bar{\psi}_e(\vec{r}, \vec{p}_e) e^{-i\vec{r}\cdot\vec{p}_e} \varphi_e(r) . \tag{8}$$

This function will be discussed in detail in the next section.

III. ELECTRON WAVE FUNCTIONS FOR A UNIFORMLY CHARGED NUCLEUS

The wave function for an electron moving in the field of a uniformly charged nucleus with radius ρ is⁷

$$\psi_e^{\mu}(\vec{r}) = \begin{pmatrix} g_{\kappa}(r) \chi_{\kappa}^{\mu}(\hat{r}) \\ i f_{\kappa}(r) \chi_{-\kappa}^{\mu}(\hat{r}) \end{pmatrix} . \tag{9}$$

Here, χ_{κ}^{μ} is the electron spin function and g_{κ} and f_{κ} are the radial wave functions. For $r \geq \rho$, the regular solutions for g_{κ} and f_{κ} are

$$\begin{aligned}
\begin{pmatrix} g_{\kappa}^0(r) \\ f_{\kappa}^0(r) \end{pmatrix} &= \pm \left[\frac{W \pm 1}{W} \right]^{1/2} \frac{|\Gamma(\gamma + iy)|}{\Gamma(2\gamma + 1)} \frac{(2pr)^{\gamma}}{r} \\
&\times e^{(1/2)\pi y} \begin{Bmatrix} \text{Re}(\Lambda) \\ \text{Im}(\Lambda) \end{Bmatrix} ,
\end{aligned} \tag{10}$$

where

$$\Lambda = (\gamma + iy) e^{i(\eta_{\kappa} - pr)} {}_1F_1(\gamma + 1 + iy, 2\gamma + 1, 2ipr) ,$$

$$p = (W^2 - 1)^{1/2} ,$$

$$\gamma_{\kappa} = [\kappa^2 - (\alpha Z)^2]^{1/2} ,$$

$$y = \alpha Z W / p ,$$

$$\exp(2i\eta_{\kappa}) = -(\kappa - i\alpha Z / p) / (\gamma + iy) ,$$

with α the fine structure constant and Z the nuclear charge. The irregular solutions for g_{κ} and f_{κ} can be obtained from Eq. (10) by replacing γ by $-\gamma$

$$\begin{pmatrix} g_{\kappa}^0(r) \\ f_{\kappa}^0(r) \end{pmatrix} \begin{matrix} \gamma \rightarrow -\gamma \\ \rightarrow \end{matrix} \begin{pmatrix} \bar{g}_{\kappa}^0(r) \\ \bar{f}_{\kappa}^0(r) \end{pmatrix} . \tag{11}$$

In order to obtain a plane wave at infinity, the asymptotic behavior of g and f must be⁸

$$\begin{cases} g_{\kappa}^0(r) \\ f_{\kappa}^0(r) \end{cases} \rightarrow \pm \left[\frac{W+1}{W} \right]^{1/2} \begin{cases} [\cos(pr+y \ln 2pr + \delta_{\kappa})] \\ [\sin(pr+y \ln 2pr + \delta_{\kappa})] \end{cases}, \quad \delta_{\kappa} = -\arg\Gamma(\gamma_{\kappa}+iy) + \eta_{\kappa} - \frac{\pi\gamma_{\kappa}}{2}. \quad (12)$$

The solution outside the nucleus is a linear combination of the regular and irregular solutions,

$$\begin{Bmatrix} g_{\kappa}(r) \\ f_{\kappa}(r) \end{Bmatrix} = B \begin{Bmatrix} g_{\kappa}^0(r) \\ f_{\kappa}^0(r) \end{Bmatrix} + H \begin{Bmatrix} \bar{g}_{\kappa}^0(r) \\ \bar{f}_{\kappa}^0(r) \end{Bmatrix}. \quad (13)$$

For $r \leq \rho$, we expand f_{κ} and g_{κ} in a power series:

$$g_{\kappa}^i(r) = \sum_n a_n r^n, \quad f_{\kappa}^i(r) = \sum_n b_n r^n. \quad (14)$$

The coefficients a_n and b_n satisfy the recurrence relations

$$\begin{aligned} a_n &= \frac{1}{n+\kappa+1} \left\{ \left[W+1 + \frac{3}{2} \frac{\alpha Z}{\rho} \right] b_{n-1} - \frac{1}{2\rho^2} \frac{\alpha Z}{\rho} b_{n-3} \right\}, \\ b_n &= \frac{1}{n-\kappa+1} \left\{ - \left[W-1 + \frac{3}{2} \frac{\alpha Z}{\rho} \right] a_{n-1} + \frac{1}{2\rho^2} \frac{\alpha Z}{\rho} a_{n-3} \right\}. \end{aligned} \quad (15)$$

The continuity of the solution at $r=\rho$ requires that a phase Δ_{κ} be added to g_{κ} and f_{κ} . The expression for Δ_{κ} is given in the Appendix. Using the continuity of the wave function at $r=\rho$, the values of g_{κ} and f_{κ} at this boundary are

$$\begin{aligned} g_{\kappa}(\rho) &= [1 + H^2 + 2H \cos(\delta_{\kappa} - \bar{\delta}_{\kappa})]^{1/2} \left[\frac{f^0(\rho)/g^0(\rho) - \bar{f}^0(\rho)/\bar{g}^0(\rho)}{f^i(\rho)/g^i(\rho) - \bar{f}^0(\rho)/\bar{g}^0(\rho)} \right] \frac{g_{\kappa}^0(\rho)}{\bar{g}_{\kappa}^0(\rho)}, \\ f_{\kappa}(\rho) &= \frac{f_{\kappa}^i(\rho)}{g_{\kappa}^i(\rho)} g_{\kappa}(\rho), \\ H &= \left[\frac{f^0(\rho)/g^0(\rho) - f^i(\rho)/g^i(\rho)}{f^i(\rho)/g^i(\rho) - \bar{f}^0(\rho)/\bar{g}^0(\rho)} \right] \frac{g_{\kappa}^0(\rho)}{\bar{g}_{\kappa}^0(\rho)}. \end{aligned} \quad (16)$$

From Eq. (16), the interior wave functions are

$$\begin{aligned} g_{\kappa}(r) &= [g_{\kappa}(\rho)/g_{\kappa}^i(\rho)] g_{\kappa}^i(r), \\ f_{\kappa}(r) &= [f_{\kappa}(\rho)/f_{\kappa}^i(\rho)] f_{\kappa}^i(r), \end{aligned} \quad (17)$$

where $r \leq \rho$. On considering only s and p waves, the electron wave function can be written

$$\psi_e(\vec{r}, \vec{p}_e) = \frac{1}{4\pi} \left[\frac{(2\pi)^3}{m_e p_e} \right]^{1/2} \begin{Bmatrix} g_{-1} e^{-i\Delta_{-1}} + i \vec{\sigma} \cdot \vec{r} \vec{\sigma} \cdot \hat{p}_e g_{+1} e^{-i\Delta_{+1}} + i(3\hat{r} \cdot \hat{p}_e - \vec{\sigma} \cdot \hat{r} \vec{\sigma} \cdot \hat{p}_e) g_{-2} e^{-i\Delta_{-2}} \\ -i \vec{\sigma} \cdot \hat{r} f_{-1} e^{-i\Delta_{-1}} + \vec{\sigma} \cdot \vec{p}_e f_{+1} e^{-i\Delta_{+1}} + i(-i \vec{\sigma} \cdot \hat{r} + 3\hat{r} \cdot \hat{p}_e \vec{\sigma} \cdot \hat{p}_e) f_{+2} e^{-i\Delta_{+2}} \end{Bmatrix}. \quad (18)$$

From Eqs. (8) and (18), we obtain

$$\begin{aligned} \langle \bar{\psi}_e \rangle &= \int d\vec{r} \psi_e e^{i\vec{r} \cdot \vec{p}_e} \varphi(\vec{r}) \\ &= \bar{u}_e (A + B\gamma_4 + C\vec{\gamma} \cdot \vec{p}_{\bar{\nu}} + D\vec{\gamma} \cdot \vec{p}_{\bar{\nu}} \gamma_4), \end{aligned} \quad (19)$$

with

$$\begin{aligned} A &= N_+ g_{-1}^{(2)} e^{+i\Delta_{-1}} - N_+ p_{\bar{\nu}} \cos\theta g_{-2}^{(3)} e^{+i\Delta_{-2}} + N_- f_{+1}^{(2)} e^{+i\Delta_{+1}} - N_- p_{\bar{\nu}} \cos\theta f_{+2}^{(3)} e^{+i\Delta_{+2}}, \\ B &= N_+ g_{-1}^{(2)} e^{+i\Delta_{-1}} - N_+ p_{\bar{\nu}} \cos\theta g_{-2}^{(3)} e^{+i\Delta_{-2}} - N_- f_{+1}^{(2)} e^{+i\Delta_{+1}} + N_- p_{\bar{\nu}} \cos\theta f_{+2}^{(3)} e^{+i\Delta_{+2}}, \\ C &= -\frac{i}{3} N_+ p_{\bar{\nu}} f_{-1}^{(3)} e^{+i\Delta_{-1}} - \frac{i}{3} N_+ p_{\bar{\nu}} f_{+2}^{(3)} e^{+i\Delta_{+2}} - \frac{i}{3} N_- p_{\bar{\nu}} g_{+1}^{(3)} e^{+i\Delta_{+1}} + \frac{i}{3} N_- p_{\bar{\nu}} g_{-2}^{(3)} e^{+i\Delta_{-2}}, \\ D &= \frac{i}{3} N_+ p_{\bar{\nu}} f_{-1}^{(3)} e^{+i\Delta_{-1}} + \frac{i}{3} N_+ p_{\bar{\nu}} f_{+2}^{(3)} e^{+i\Delta_{+2}} - \frac{i}{3} N_- p_{\bar{\nu}} g_{+1}^{(3)} e^{+i\Delta_{+1}} + \frac{i}{3} N_- p_{\bar{\nu}} g_{-2}^{(3)} e^{+i\Delta_{-2}}, \end{aligned}$$

and

$$\begin{aligned} N_{\pm} &= \frac{3}{4\pi p^3} \left[\frac{(2\pi)^3}{m_e p_e} \right]^{1/2} \left[\frac{m_e}{2(W \pm p_e)} \right]^{1/2}, \\ g_{\kappa}^{(m)} &= \int_{r=0}^{\rho} dr r^m g_{\kappa}(r), \quad f_{\kappa}^{(m)} = \int_{r=0}^{\rho} dr r^m f_{\kappa}(r). \end{aligned}$$

In deriving Eq. (19), we use the approximations

$$\begin{aligned} r p_{\bar{\nu}} \sin(r p_{\bar{\nu}}) &\simeq (r p_{\bar{\nu}})^2, \\ (r p_{\bar{\nu}}) \cos(r p_{\bar{\nu}}) - \sin(r p_{\bar{\nu}}) &\simeq -\frac{1}{3} (r p_{\bar{\nu}})^3. \end{aligned}$$

IV. BETA DECAY TRANSITION RATE

In order to compute the beta decay transition rate, it is convenient to introduce the nuclear part, h_{α} , and the leptonic part, l_{α} , of the matrix element as

$$\begin{aligned} h_{\alpha} &= \langle f(\vec{p}_f) | J_{\alpha}^{(+)}(0) | i(\vec{p}_i) \rangle, \\ l_{\alpha} &= \langle \bar{\psi}_e \rangle \gamma_{\alpha} (1 + \gamma_5) v_{\bar{\nu}}(\vec{p}_{\bar{\nu}}), \\ &= \bar{u}_e (A + B\gamma_4 + C\vec{\gamma} \cdot \hat{r} + D\vec{\gamma} \cdot \hat{r} \gamma_4) \\ &\quad \times \gamma_{\alpha} (1 + \gamma_5) v_{\bar{\nu}}(\vec{p}_{\bar{\nu}}). \end{aligned} \quad (20)$$

With these definitions, Eq. (1) can be written

$$\begin{aligned} \mathcal{M} &= \frac{G \cos\theta_C}{\sqrt{2}} (2\pi)^3 \delta^{(3)}(\vec{p}_i - \vec{p}_f - \vec{p}_e - \vec{p}_{\bar{\nu}}) \\ &\quad \times \sum_{\alpha} h_{\alpha} l_{\alpha}. \end{aligned} \quad (21)$$

The rate is then obtained by squaring the matrix element, Eq. (21), summing over final spins, averaging over the initial spin, and multiplying by the phase space to obtain

$$\begin{aligned} d\omega &= \frac{G^2 \cos^2\theta_C}{2} \frac{1}{(2\pi)^5} \int \delta^{(4)}(p_i - p_f - p_e - p_{\bar{\nu}}) \\ &\quad \times \frac{1}{2} \sum_{S_i S_f S_e S_{\bar{\nu}}} h_{\alpha} h_{\beta}^* l_{\alpha} l_{\beta}^* \\ &\quad \times d\vec{p}_f d\vec{p}_{\bar{\nu}} d\vec{p}_e. \end{aligned} \quad (22)$$

Given the complicated forms of h_{α} and l_{α} , the spin sums, which result in traces of Dirac matrices, are ordinarily tedious to evaluate. We have performed a complete evaluation of the squared matrix element by using the algebraic manipulation program SCHOONSCHIP developed by Veltman.⁹ The calculation was performed retaining terms proportional to the square of the weak magnetic form factor F_M . The expression for the differential transition probability is sufficiently long that the results are most conveniently displayed graphically. We restrict ourselves to various graphs of contributions to the beta spectrum after integrations over the recoiling nu-

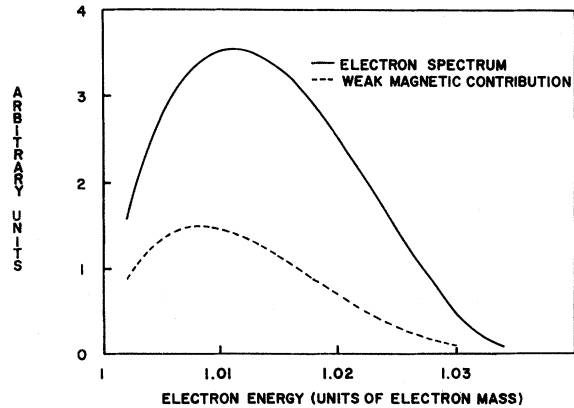


FIG. 1. Electron spectrum in arbitrary units. The lower curve represents 2×10^4 times the weak magnetic contribution. The energy is measured in electron masses.

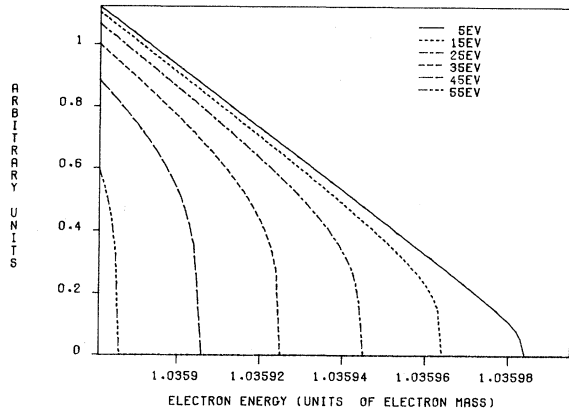


FIG. 2. End points of the Kurie plot for various values of the neutrino mass between 0 and 55 eV.

cleus and neutrino variables have been performed numerically. The results for the beta spectrum, the weak magnetic contribution to the spectrum, the Kurie plot, and the effective Kurie plot for a spectrum containing a mixture of atomic excitations in the final state are shown in Figs. 1–3. Special attention is given to the effect of the neutrino mass on the end point.

V. DISCUSSION AND SUMMARY

The elementary particle treatment of nuclear beta decay provides a convenient formalism within which to discuss neutrino mass effects. We have applied this formalism to the case of tritium beta decay in order to assess how known corrections to the beta

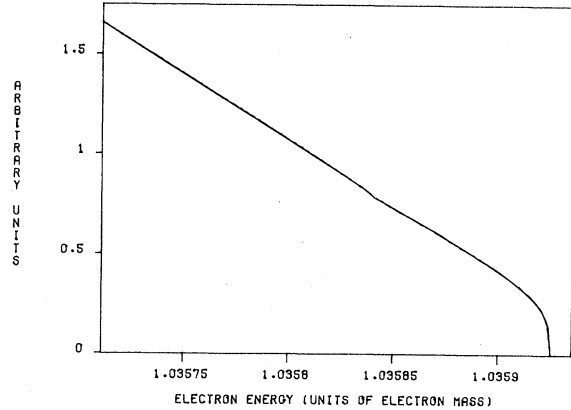


FIG. 3. Kurie plot in the case of a mixture of 70% ground state and 30% atomic excited state for the daughter nuclei.

spectrum are influenced by a nonzero value of m_ν . We find that weak magnetism contributes at the part in 10^5 level, which is probably not sufficiently large to affect the determination of m_ν . Similarly, contributions to the electron wave function corresponding to values of the orbital angular momentum $l > 0$ do not have a significant effect on the beta spectrum of light nuclei.

However, the combination of the Coulomb corrections in the elementary particle formalism and nuclear recoil effects does produce changes in the simplest theoretical description of the Kurie plot. In order to characterize these differences, we have made a fit of our calculated *theoretical* Kurie plot to the function

$$K = A \frac{(\Delta - E_e)^{1/2}}{\left[1 - \frac{2E_e}{M_i} + \frac{m_e^2}{M_i^2}\right]} \left[(\Delta - E_e)^2 - m_\nu^2 \left[1 - \frac{2E_e}{M_i} + \frac{m_e^2}{M_i^2}\right] \right]^{1/4} \left[1 - \frac{E_e}{M_i}\right]^{1/2} \left[1 - a \frac{m_\nu}{m_e} \frac{E_0 - \bar{E}_e}{E_0 - E_e}\right], \quad (23)$$

where

$$\Delta = \frac{1}{2M_i} (M_i^2 - M_f^2 + m_e^2 + m_\nu^2); \quad E_0 = M_i - M_f; \quad \bar{E}_e = E_{e,\max}.$$

The factors preceding the final square bracket represent the exact Kurie plot under the assumption that the nuclear matrix element is constant. This assumption proves to be quite reasonable, since the constant matrix element Kurie plot differs from the calculated Kurie plot by only a percent or so for neutrino masses in the range 0 to 55 eV. By way of comparison, the Kurie plot obtained by assuming no recoil differs from our calculated result by more than 5% over the same range of neutrino masses.

These comparisons show that nuclear recoil is the main correction to the end point for light nuclei. We have attempted to characterize the remaining corrections by a single parameter a which has its maximum effect at the end point and decreases as the linear region of the Kurie plot is approached. For $a=100$, the departure of the fitted spectrum from the calculated weak spectrum ranges from 0.8% for a neutrino mass of 55 eV to 0.1% for a neutrino mass of 5 eV. The fits were made in the re-

gion of electron energies within 1 keV from the end point.

For completeness, Fig. 3 shows a Kurie plot for the case when the daughter nucleus consists of a mixture of the ground state and an atomic excited state. Notice that there is a discernible break in the Kurie plot near the excitation energy of the atomic level.

To summarize, we have included corrections to the tritium beta decay spectrum which could influence the determination of the neutrino mass. Apart from possible effects associated with the emission of real photons, the major corrections involve nuclear recoil and the presence of atomic excited states of

the daughter nucleus. Our calculations incorporate these effects to an accuracy of an eV.

ACKNOWLEDGMENTS

We have benefited from a number of conversations with Prof. Hamish Robertson, Prof. J. Hetherington, and Prof. David Yen. One of us (C.W.) wishes to thank the Physics Department of Michigan State University for its hospitality while this work was being performed. This research was supported in part by the National Science Foundation under grant PHY 8105020.

APPENDIX

The phase introduced in Eq. (22) has the form⁵

$$\tan\Delta_\kappa = \frac{-a_0 + a_1 \tan\eta_\kappa + H_\kappa \left[\frac{\cos\bar{\eta}_\kappa}{\cos\eta_\kappa} \right] (a_2 + a_3 \tan\bar{\eta}_\kappa)}{a_1 + a_0 \tan\eta_\kappa + H_\kappa \left[\frac{\cos\bar{\eta}_\kappa}{\cos\eta_\kappa} \right] (a_3 - a_2 \tan\bar{\eta}_\kappa)},$$

where

$$\begin{aligned} \tan\eta_\kappa &= \frac{\alpha Z}{p} \frac{W-1}{\kappa-\gamma_\kappa}, \quad \tan\bar{\eta}_\kappa = \frac{\alpha Z}{p} \frac{W-1}{\kappa+\gamma_\kappa}, \\ a_0 &= \sin \frac{\pi\gamma_\kappa}{2} \operatorname{Re} \frac{\Gamma(\gamma_\kappa+iy)}{|\Gamma(\gamma_\kappa+iy)|} + \cos \frac{\pi\gamma_\kappa}{2} \operatorname{Im} \frac{\Gamma(\gamma_\kappa+iy)}{|\Gamma(\gamma_\kappa+iy)|}, \\ a_1 &= \cos \frac{\pi\gamma_\kappa}{2} \operatorname{Re} \frac{\Gamma(\gamma_\kappa+iy)}{|\Gamma(\gamma_\kappa+iy)|} - \sin \frac{\pi\gamma_\kappa}{2} \operatorname{Im} \frac{\Gamma(\gamma_\kappa+iy)}{|\Gamma(\gamma_\kappa+iy)|}, \\ a_2 &= \sin \frac{\pi\gamma_\kappa}{2} \operatorname{Re} \frac{\Gamma(-\gamma_\kappa+iy)}{|\Gamma(-\gamma_\kappa+iy)|} - \cos \frac{\pi\gamma_\kappa}{2} \operatorname{Im} \frac{\Gamma(-\gamma_\kappa+iy)}{|\Gamma(-\gamma_\kappa+iy)|}, \\ a_3 &= \cos \frac{\pi\gamma_\kappa}{2} \operatorname{Re} \frac{\Gamma(-\gamma_\kappa+iy)}{|\Gamma(-\gamma_\kappa+iy)|} + \sin \frac{\pi\gamma_\kappa}{2} \operatorname{Im} \frac{\Gamma(-\gamma_\kappa+iy)}{|\Gamma(-\gamma_\kappa+iy)|}. \end{aligned}$$

The phase factor difference is given by

$$\exp\{i(\Delta_\kappa - \Delta_{\kappa'})\} = \frac{\pm 1}{[(1 + \tan^2\Delta_\kappa)(1 + \tan^2\Delta_{\kappa'})]^{1/2}} \{(1 + \tan\Delta_\kappa \tan\Delta_{\kappa'}) + i(\tan\Delta_\kappa - \tan\Delta_{\kappa'})\}.$$

The plus sign is used when $|\kappa| = |\kappa'|$, while the minus sign is used when $|\kappa| \neq |\kappa'|$.

*Permanent address: Guangxi University, Nanning, Guangxi, People's Republic of China.

¹R. G. H. Robertson *et al.*, in Proceedings of the 1982 Conference on Neutrinos, Balaton, Hungary, 1982, Los Alamos National Laboratory Report No. LA-UR-82-1728, 1982. For other discussions of tritium beta decay and neutrino mass effects, see K-E. Bergkvist, Nucl.

Phys. **B39**, 266 (1972); J. J. Simpson, Phys. Rev. D **23**, 649 (1981); J. Law, Phys. Lett. **102B**, 371 (1982).

²V. A. Lubimov, E. G. Novikov, V. Z. Nozik, E. F. Tretyakov, and V. S. Kosik, Phys. Lett. **94B**, 266 (1980).

³C. W. Kim and H. Primakoff, Phys. Rev. **139**, B1447 (1965); **140**, B566 (1965).

⁴L. Armstrong and C. W. Kim, Phys. Rev. C **5**, 672

- (1972).
- ⁵C. P. Bhalla and M. E. Rose, Phys. Rev. 128, 774 (1962); Oak Ridge National Laboratory Report 3207, 1962; J. N. Huffaker and C. E. Laird, Nucl. Phys. A93, 584 (1967).
- ⁶C. W. Kim, Nuovo Cimento 4, 189 (1974).
- ⁷M. E. Rose, *Relativistic Electron Theory* (Wiley, New York, 1961).
- ⁸E. Konopinski, *The Theory of Beta Radioactivity* (Oxford Press, London, 1966).
- ⁹H. Strubbe, Comput. Phys. Commun. 8, 1 (1974).